

## The Effect of Stress Wave Dispersion on the Drivability Analysis of Large-Diameter Monopiles

Meijers, Peter; Tsouvalas, Apostolos; Metrikine, Andrei

**DOI**

[10.1016/j.proeng.2017.09.272](https://doi.org/10.1016/j.proeng.2017.09.272)

**Publication date**

2017

**Document Version**

Final published version

**Published in**

X International Conference on Structural Dynamics, EURODYN 2017

**Citation (APA)**

Meijers, P., Tsouvalas, A., & Metrikine, A. (2017). The Effect of Stress Wave Dispersion on the Drivability Analysis of Large-Diameter Monopiles. In F. Vestroni, V. Gattulli, & F. Romeo (Eds.), *X International Conference on Structural Dynamics, EURODYN 2017* (Vol. 199, pp. 2390-2395). (Procedia Engineering; Vol. 2017, No. 199). <https://doi.org/10.1016/j.proeng.2017.09.272>

**Important note**

To cite this publication, please use the final published version (if applicable). Please check the document version above.

**Copyright**

Other than for strictly personal use, it is not permitted to download, forward or distribute the text or part of it, without the consent of the author(s) and/or copyright holder(s), unless the work is under an open content license such as Creative Commons.

**Takedown policy**

Please contact us and provide details if you believe this document breaches copyrights. We will remove access to the work immediately and investigate your claim.



X International Conference on Structural Dynamics, EURODYN 2017

# The Effect of Stress Wave Dispersion on the Drivability Analysis of Large-Diameter Monopiles

P.C. Meijers<sup>a,\*</sup>, A. Tsouvalas<sup>a</sup>, A.V. Metrikine<sup>a</sup>

<sup>a</sup>Faculty of Civil Engineering and Geosciences, Delft University of Technology, Stevinweg 1, 2628 CN Delft, The Netherlands

---

## Abstract

Due to the increasing need for energy from renewable resources, a large number of offshore wind farms are planned to be constructed in the near future. Despite the plethora of available foundation concepts for offshore wind turbines, the monopile foundation is the most widely adopted concept in practice. To predict the installation process for a monopile a so-called drivability study is performed. Such a study allows one to decide on a number of key parameters for the installation process, such as, the appropriate size of the hydraulic hammer, the number of hammer blows and energy input needed to reach the final penetration depth, and the induced stresses in the system. The latter is important for the prediction of the fatigue life of the pile.

Currently, drivability studies are based on one-dimensional wave equation models as first proposed by Smith in the 1950s. These models are valid as long as the diameter of the pile is small compared to the excited wavelengths in the structure due to the hammer impact. For large-diameter monopiles that are currently being used in the offshore wind industry, the latter condition is not met and the effect of stress wave dispersion can no longer be neglected.

In this paper the classical wave equation model is amended by an extra term which accounts for the lateral inertia of the cross-section, resulting in the so-called Rayleigh-Love rod theory. With this new model, a parametric study is performed in which the effect of stress wave dispersion on the induced stresses and the number of hammer blows needed to reach the final penetration depth are assessed. A comparison with the results obtained from the classical model is also included in order to define the applicability range of the models. It is shown that the effect of stress wave dispersion can not be neglected for a drivability study of large-diameter monopiles.

© 2017 The Authors. Published by Elsevier Ltd.

Peer-review under responsibility of the organizing committee of EURODYN 2017.

*Keywords:* Monopile foundation, drivability study, lateral inertia, wave equation, stress wave dispersion, offshore wind energy

---

## 1. Introduction

Due to the increasing need for energy from renewable resources, a large number of offshore wind farms are planned to be constructed in the near future. To accommodate wind turbines of larger capacity, the size of the support structures is increased. The most commonly used support structure is a steel monopile [1]. Recently installed monopiles in the North Sea reached a diameter of about 8 m and a length of over 80 m [2]. The dimensions are expected to increase in the coming years as larger and more powerful wind turbines are designed.

---

\* Corresponding author. Tel.: +31-15-27-85260

E-mail address: [p.c.meijers@tudelft.nl](mailto:p.c.meijers@tudelft.nl)

Monopiles are driven into the seabed in various ways. The most commonly used technique is to drive the pile to the desired penetration depth with a hydraulic hammer. In order to determine the hammer type and the number of blows needed to reach the final penetration depth a so called drivability study is performed. The induced stresses in the structure are also computed as a prerequisite for an estimation of the fatigue damage inflicted by the pile driving process [3]. Since fatigue damage depends on the number of stress cycles and their amplitudes, an accurate prediction of the stress history during pile driving is of importance.

A drivability study is often performed using a wave analysis program such as GRLWEAP [4], which is based on the one-dimensional wave equation model developed by Smith in the 1950s [5]. The resistance of the soil is usually modelled with non-linear springs and dashpots representing the soil stiffness and damping respectively. To improve the predictions of original model by Smith, several additional models have been introduced over the years, as for example the ones by Randolph and Simons [6] and Lee et al. [7]. In parallel, more advanced models have also been developed through the years which are primarily based on the use of the Finite Element Method (FEM) to describe the soil together with a three-dimensional description of the structure [8,9]. Despite the fact that such models are expected to increase the accuracy of the predictions, they are computationally expensive, hence, they never actually replaced the original model by Smith.

The original drivability model developed by Smith is based on the classical one-dimensional wave equation in which geometrical dispersion effects are neglected. For slender piles in which the excited wavelengths in the system are much longer compared to the pile diameter such effects can indeed be neglected. However, for larger-size monopiles excited at relatively low frequencies dispersive effects can be quite significant around the ring frequency of the cylindrical shell structure. In his PhD-thesis, Deeks [9] concludes that for thin-walled piles stress wave dispersion is present and that further research is needed. In the more recent work by Deng et al. [10], it is mentioned that the simple one-dimensional model is not capable of describing accurately the stress wave propagation in large-diameter piles during pile driving.

In this paper a simple extension of the one-dimensional drivability model is proposed to include the geometrical dispersion effects associated with large-diameter monopiles used in industry today. A parametric study is conducted to reveal the applicability range of the various models. Finally, conclusions are reached as to the influence of the geometrical dispersion in the stress wave propagation along the pile and the possible influence in the pile driving process.

## 2. Drivability model

A sketch of the pile driving process is shown in Fig. 1. A linear elastic cylindrical hollow pile is partially embedded into a uniform soil layer. The pile is considered to be thin-walled with outer radius  $r$ , wall thickness  $h$  and cross-sectional area  $A \approx 2\pi rh$ . The material properties of the pile are Young's modulus  $E$ , Poisson's ratio  $\nu$  and density  $\rho$ , whereas soil properties are similar but have the subscript  $s$ . To prevent soil plugging in the pile, which would complicate the analysis, the tip of the pile is considered to be closed by a round plate.

The displacement of the pile,  $u(z, t)$ , is assumed to be governed by the Rayleigh-Love rod theory [11, p. 116-121], which is an improvement of the classical rod theory to include the effect of lateral inertia of the cross-section. The governing equation is

$$\rho A \frac{\partial^2 u}{\partial t^2} - EA \frac{\partial^2 u}{\partial z^2} + R_s - \left[ \rho \nu^2 I_p \frac{\partial^4 u}{\partial t^2 \partial z^2} \right] = 0, \quad (1)$$

in which  $R_s$  is the non-linear resistance of the soil and  $I_p$  is the polar second momentum of area of the cross-section. The term in square brackets is the additional Rayleigh-Love correction term, which is not included in the original wave equation model by Smith [5].

From the displacement  $u(z, t)$ , the axial stress  $\sigma(z, t)$  in the pile can be computed as

$$\sigma(z, t) = E \frac{\partial u}{\partial z} + \left[ \nu^2 r_g^2 \frac{\partial^3 u}{\partial t^2 \partial z} \right],$$

where  $r_g = \sqrt{I_p/A}$  is the radius of gyration. Again, the term between square brackets emerges from the Rayleigh-Love theory and is neglected in classical wave equation approach.

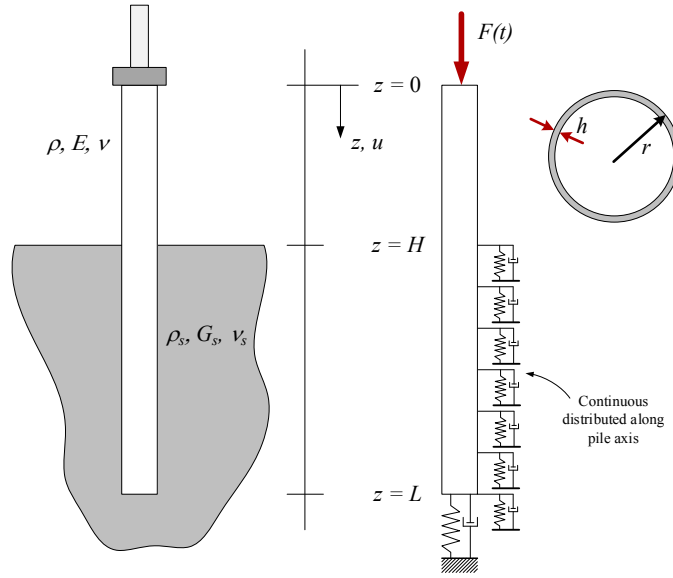


Fig. 1. Sketch of the pile driving process (left) and the drivability model (right).

At  $t = 0$  the system is assumed to be at rest and the boundary conditions are given by

$$\sigma(0, t) = F(t)/A, \tag{2}$$

$$\sigma(L, t) = P_s/A, \tag{3}$$

where  $F(t)$  is the hammer force and  $P_s$  the soil response at the pile tip.

The soil is modelled by distributed non-linear springs and dashpots, following the classical approach of Randolph and Simons [6]. This model has been developed originally for piles of relatively small diameter and assumes a local reaction of the soil. In equation (1), the soil resistance along the pile shaft per unit length of the pile,  $R_s$ , is given by

$$R_s = \begin{cases} K_s u + C_s \frac{\partial u}{\partial t} & \text{when } |K_s u + C_s \frac{\partial u}{\partial t}| < 2\pi r q_u, \\ 2\pi r q_u & \text{otherwise,} \end{cases}$$

where the soil stiffness  $K_s = 2.9G_s$  and the soil damping  $C_s = 2\pi r \sqrt{G_s \rho_s}$ , in which  $G_s$  is the shear modulus and  $\rho_s$  is the density of the soil. The magnitude of the soil resistance is limited by the ultimate friction coefficient  $q_u$  of the soil multiplied by the circumference of the pile.

Similarly, the soil response at the pile tip ( $P_s$  in equation (3)) is given by

$$P_s = \begin{cases} K_t u + C_t \frac{\partial u}{\partial t} & \text{when } |K_t u| < A_t P_s^{\max}, \\ A_t P_s^{\max} + C_t \frac{\partial u}{\partial t} & \text{otherwise,} \end{cases}$$

where  $K_t = 4G_s r / (1 - \nu_s)$  and  $C_t = 3.4r^2 \sqrt{G_s \rho_s} / (1 - \nu_s)$  with  $\nu_s$  the Poisson's ratio of the soil. Furthermore,  $P_s^{\max}$  is the ultimate soil resistance and  $A_t = \pi r^2$  is the cross-sectional area of the pile tip. The final set of the pile after one hammer blow is equal to the displacement of the pile head when the system is at rest again.

### 3. Cases

To investigate the effect of lateral inertia on the stress wave dispersion, predictions of a classical wave equation model [6] are compared with the results of the present model for three different cases. The cases consider piles of different radii while keeping induced stress levels and frequency content of the hammer force equal. The numerical values used for all piles are presented in Table 1 and case specific quantities are provided in Table 2.

Table 1. Pile and soil properties used for all cases

Pile parameter	Value	Soil parameter	Value	Soil parameter	Value
$E$	210 GPa	$G_s$	24.25 GPa	$q_u$	100 kN/m <sup>2</sup>
$\nu$	0.3	$\nu_s$	0.48	$p_s^{\max}$	900 kN/m <sup>2</sup>
$\rho$	7750 kg/m <sup>3</sup>	$\rho_s$	1900 kg/m <sup>3</sup>		
$L$	58 m	$H$	23 m		

Table 2. Case specific parameters and values for the final set of the pile after a single hammer blow

Case	$r$ [m]	$h$ [mm]	$\alpha$ [-]	$f_r$ [Hz]	$\tilde{f}$ [-]	$u_{CW}$ [mm]	$u_{RL}$ [mm]	$\Delta u$ [%]
1	0.4572	20	1.0	1900	0.23	5.57	5.55	-0.36
2	2.0	40	8.75	434	1.00	6.00	6.02	0.33
3	3.5	70	26.8	248	1.73	5.64	5.87	4.08

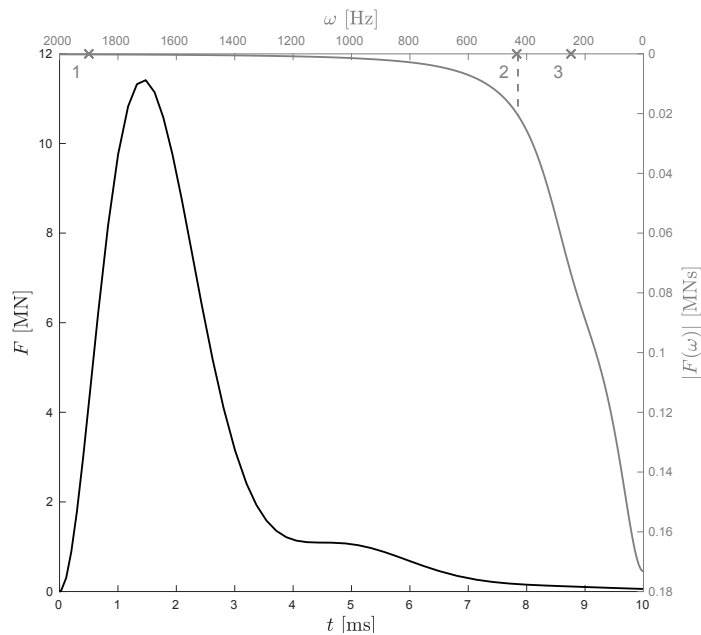


Fig. 2. Time signal of the input force for Case 1 (small pile) in black. The corresponding amplitude spectrum is shown in gray, with  $f_{90} = 430$  Hz indicated by the vertical dashed line. The ring frequencies for the three considered cases are indicated with an x.

The hammer force  $F(t)$  in equation (2) for Case 1 is generated using the hammer model developed by Deeks and Randolph [12] with  $m_r = 4000$  kg,  $m_a = 1000$  kg,  $c_c = 0$  Ns/m,  $k_c = 3.5$  GN/m,  $v_0 = 6.5$  m/s,  $Z = A\sqrt{E\rho} = 2.3$  MNs/m. The resulting time signal is shown in Fig. 2 together with the amplitude spectrum of the signal,  $|F(\omega)|$ . In Fig. 2, the upper bound of the frequency range containing 90% of the energy,  $f_{90}$ , is indicated. This characteristic frequency is defined as

$$\int_0^{f_{90}} |F(\omega)| d\omega = 0.9 \int_0^{\infty} |F(\omega)| d\omega.$$

In order to keep the frequency content (and therefore  $f_{90}$ ) of the hammer force equal for the three cases, only the amplitude of the force signal is scaled with scaling parameter  $\alpha$  as presented in Table 2. The magnitude of  $\alpha$  is chosen such that the stresses induced at the pile head are equal for all cases.

A characteristic for the wave propagation in a monopile is the ring frequency. This frequency corresponds with the breathing mode of the cylindrical shell structure and is given by [13]

$$f_r = \frac{1}{2\pi r} \sqrt{\frac{E}{\rho(1-\nu^2)}}.$$

For larger radii, the value of the ring frequency decreases, as can be seen in Table 2. By defining the dimensionless frequency

$$\bar{f} = \frac{f_{90}}{f_r},$$

an indication is given whether the ring frequency of the pile lies outside ( $\bar{f} < 1$ ) or within ( $\bar{f} > 1$ ) the energy containing frequency range of the force signal.

#### 4. Numerical set-up

The problem defined above is solved numerically by means of the Finite Element Method using FEniCS [14]. The pile is divided into 250 linear elements, resulting in  $\Delta x = 0.232$  m. An explicit Newmark time marching scheme ( $\beta = 0.25$  and  $\gamma = 0.5$ ) [15] with a time step of  $\Delta t = 1 \cdot 10^{-5}$  s is chosen for the time integration of the governing equations.

#### 5. Discussion

The axial stress distributions of the incident wave ( $t = 0.10$  s, black) and the reflected wave ( $t = 0.21$  s, gray) are shown in Fig. 3 for the three cases. For  $\bar{f} < 1$  the stress profiles predicted by both models do not differ from each other. When  $\bar{f} \approx 1$  the profiles start to differ: the shape is similar, but a time shift is observed. Due to the similarity in stress wave shape, fatigue predictions for this case will not differ when the classical model or the proposed model is used since the number of stress cycles does not change. However, for  $\bar{f} > 1$ , the dispersion of the stress wave as a result of lateral inertia, is no longer negligible. A careful examination of the presented stress wave profiles shows that the dispersion causes additional alterations of compressive and tensile stresses in the pile compared to the classical approach. This means that number of stress cycles increases. Therefore, predictions of consumed fatigue life of the pile based on the new model will be higher.

A drivability study is also used to predict the penetration of the pile into the soil due to a single hammer blow, giving an indication of the total number of impacts needed to reach the desired penetration depth. The pile set from one hammer blow determined with both models is presented in Table 2 for each of the three cases. The difference between the predicted set of the classical model ( $u_{CW}$ ) and of the dispersive model ( $u_{RL}$ ) is also given as a percentage of  $u_{CW}$ . When the shape of the stress wave is similar (case 1 and 2,  $\bar{f} \leq 1$ ) both models predict a comparable penetration. For  $\bar{f} > 1$ , the difference between the set predicted by both models becomes larger, which results in a different prediction of the number of blows to reach the desired penetration depth.

#### 6. Conclusion

Currently, a drivability analysis ignores the stress wave dispersion caused by the lateral inertia of the cross-section, since it is based on a classical wave equation model. In this paper, the effect of lateral inertia is included by adding the Rayleigh-Love correction term to the governing equations, while the soil is modelled with distributed non-linear springs and dashpots conform to the classical approach. A case study shows that for large-diameter monopiles two aspects of the drivability analysis, the induced axial stress levels and the predicted pile set, are altered by stress wave dispersion. These two quantities are of importance for the prediction of the fatigue damage of the pile caused by the pile driving process. Therefore, the effect of lateral inertia should be considered in a drivability analysis when the ring frequency of the pile lies within the energy containing frequency range of the hammer force, i.e. when  $\bar{f} > 1$ .

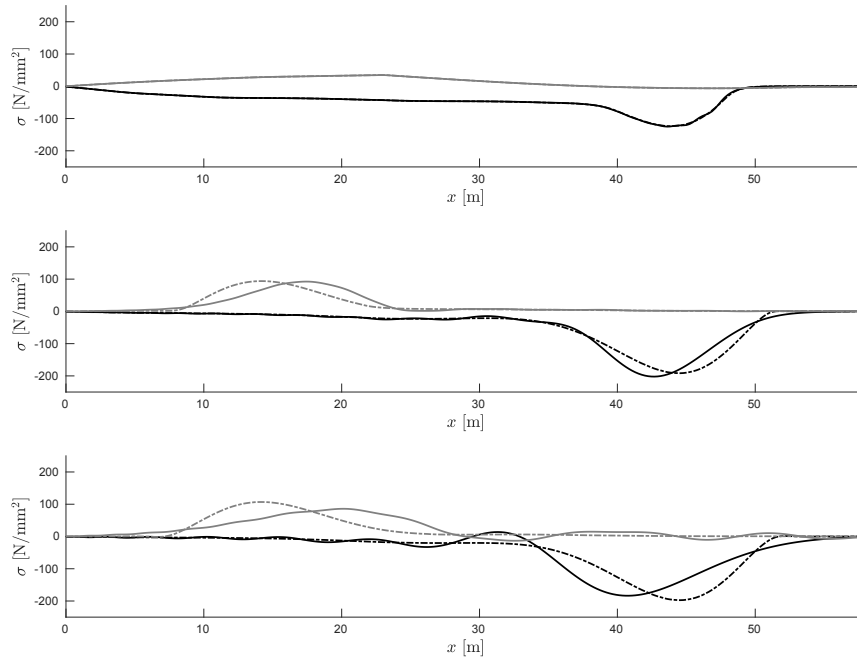


Fig. 3. Axial stress distributions along the pile axis at  $t = 0.10$  s (black) and  $t = 0.21$  s (gray) for different values of  $\bar{f}$ . The dashed lines (–) are the results from the classical wave equation model and the solid lines (–) the results from the newly proposed method. From top to bottom  $\bar{f} = 0.23$ ,  $\bar{f} = 1.00$  and  $\bar{f} = 1.73$ , respectively.

## Acknowledgements

This research is part of the EUROS programme, which is supported by NWO domain Applied and Engineering Sciences and partly funded by the Dutch Ministry of Economic Affairs.

## References

- [1] WindEurope, The European Offshore Wind Industry. Key Trends and Statistics 2016, Technical Report, WindEurope, 2017.
- [2] 4C Offshore, Veja Mate Offshore Wind Farm, <http://www.4coffshore.com/windfarms/veja-mate-germany-de36.html>, 2017. Accessed: 2017-02-17.
- [3] J. Chung, R. Wallerand, M. Hélias-Brault, Pile Fatigue Assessment During Driving, *Procedia Engineering* 66 (2013) 451–463.
- [4] PDI, Wave Equation Analysis of Pile Driving, Pile Dynamics Inc., Cleveland, Ohio, 2010.
- [5] E. A. L. Smith, Pile-driving analysis by the wave equation, *American Society of Civil Engineers Transactions* 127 (1962) 1145–1193.
- [6] M. F. Randolph, H. A. Simons, An Improved Soil Model for One-dimensional Pile Driving Analysis, in: *Méthodes Numériques de Calcul Des Pieux Pour Les Ouvrages En Mer*, 1986.
- [7] S. L. Lee, Y. K. Chow, G. P. Karunaratne, K. Y. Wong, Rational Wave Equation Model for Pile-Driving Analysis, *Journal of Geotechnical Engineering* 114 (1988) 306–325.
- [8] I. M. Smith, Y. K. Chow, Three dimensional analysis of pile drivability, in: *Proc. 2nd Int. Conf. on Numerical Methods in Offshore Piling*, Austin, Texas, 1982, pp. 1–19.
- [9] A. J. Deeks, Numerical Analysis of Pile Driving Dynamics, Ph.D. thesis, University of Western Australia, 1992.
- [10] Q. Deng, W. Jiang, W. Zhang, Theoretical investigation of the effects of the cushion on reducing underwater noise from offshore pile driving, *The Journal of the Acoustical Society of America* 140 (2016) 2780–2793.
- [11] K. F. Graff, *Wave Motion in Elastic Solids*, Courier Corporation, 1975.
- [12] A. J. Deeks, M. F. Randolph, Analytical modelling of hammer impact for pile driving, *International Journal for Numerical and Analytical Methods in Geomechanics* 17 (1993) 279–302.
- [13] A. Tsouvalas, A. V. Metrikine, A semi-analytical model for the prediction of underwater noise from offshore pile driving, *Journal of Sound and Vibration* 332 (2013) 3232–3257.
- [14] A. Logg, K.-A. Mardal, G. N. Wells, et al., *Automated Solution of Differential Equations by the Finite Element Method*, Springer, 2012.
- [15] N. M. Newmark, A Method of Computation for Structural Dynamics, *Journal of the Engineering Mechanics Division* 85 (1959) 67–94.